

AD-A138 039

ISOLATED CHARACTER RECOGNITION BASED ON
THREE-DIMENSIONAL PHASOR REPRESENTATION (U) AIR FORCE INST
OF TECH WRIGHT-PATTERSON AFB OH SCHOOL OF ENGRS

1/1

UNCLASSIFIED

D E SNYDER DEC 83 AFIT/GE0/EE-83D-8

F/G 6/4

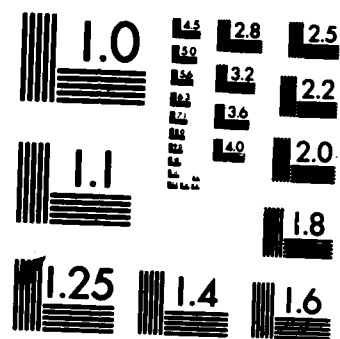
NL

END

FILED

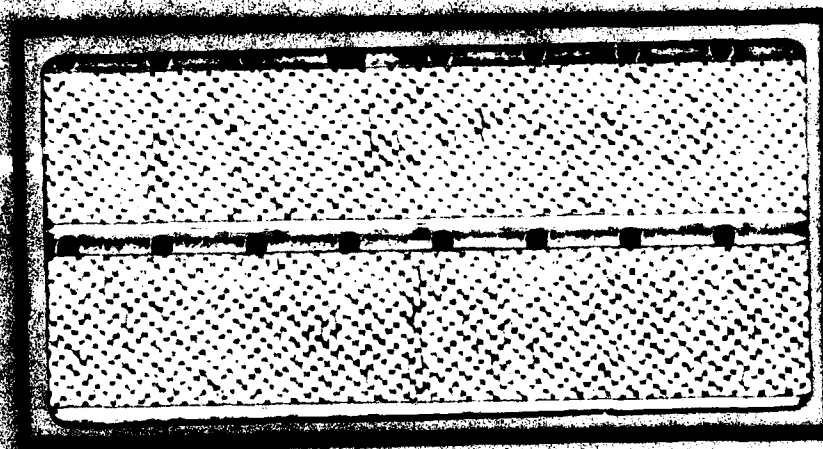
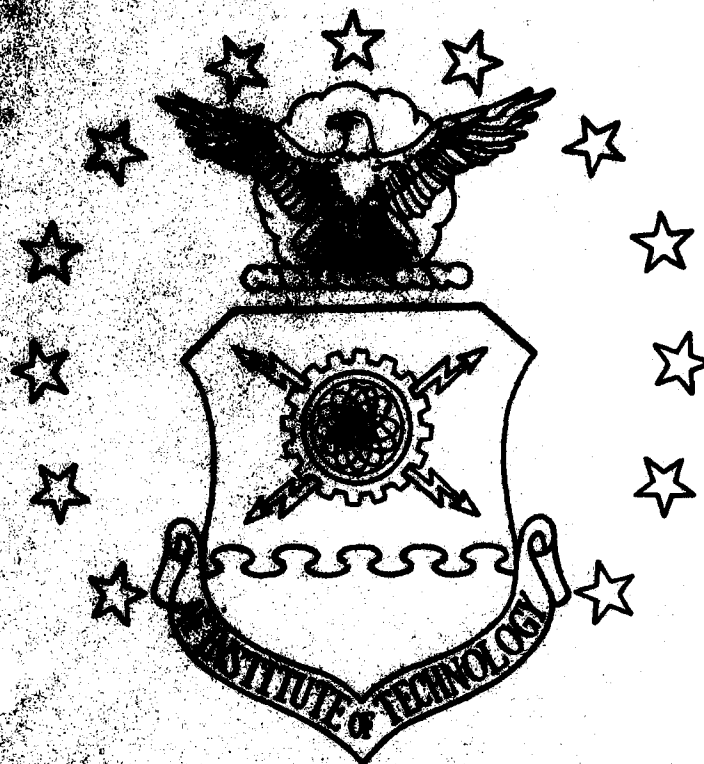
3

ATC



MICROCOPY RESOLUTION TEST CHART
NATIONAL BUREAU OF STANDARDS-1963-A

AD A138039



DTIC
ELECTE
S FEB 21 1984

D

DEPARTMENT OF THE AIR FORCE
AIR UNIVERSITY
AIR FORCE INSTITUTE OF TECHNOLOGY

Wright-Patterson Air Force Base, Ohio

DISTRIBUTION STATEMENT A

Approved for public release;
Distribution Unlimited

84 02 17 077

AFIT/GEO/EE/83D-8

Accession For	
NTIS GRA&I	<input checked="" type="checkbox"/>
DTIC TAB	<input type="checkbox"/>
Unannounced	<input type="checkbox"/>
Justification	
By	
Distribution/	
Availability Codes	
Dist	Avail and/or Special
A11	



ISOLATED CHARACTER RECOGNITION BASED ON
THREE-DIMENSIONAL PHASOR REPRESENTATION
OF SPATIAL FREQUENCY COMPONENTS

THESIS

AFIT/GEO/EE/83D-8

Daniel E. Snyder
Capt USAF

S DTIC
ELECTE
FEB 21 1984
D

Approved for public release; distribution unlimited.

ISOLATED CHARACTER RECOGNITION BASED ON
THREE-DIMENSIONAL PHASOR REPRESENTATION
OF SPATIAL FREQUENCY COMPONENTS

THESIS

Presented to the Faculty of the School of Engineering
of the Air Force Institute of Technology
Air University
in Partial Fulfillment of the
Requirements for the Degree of
Master of Science

by

Daniel E. Snyder, B.S.

Capt. USAF

Graduate Electro - Optics

December 1983

Preface

✓ This research has been motivated by the research in the area of pattern recognition by Dr. Matthew Kabrisky, Professor of Electrical Engineering, Air Force Institute of Technology. A highly efficient character recognition scheme which utilized a three-dimensional phasor representation of the spatial frequency content of an input was developed and used for pattern identification. This report contains the theory and results of this research, and recommends several areas on which future research should be based. ←

I take this opportunity to thank my advisor, Dr. Matthew Kabrisky, for providing the inspiration for this research. I would also like to thank my committee members, Major Larry R. Kizer and Dr. Vic Syed, for their valued support.

In conclusion, I thank my wife Ellen, and my son Ryan for their support, understanding, and love which made this thesis possible.

Daniel E. Snyder

Contents

	<u>Page</u>
Preface	ii
List of Figures	iv
Abstract	vi
I. Introduction	I-1
II. Human Visual System	II-1
Human Visual System as a Spatial Frequency Analyzer	-1
Modulation Transfer Function of the Human Visual System	-1
III. Fourier Analysis	III-1
Overview of Fourier Analysis	-1
DFT of a Two-Dimensional Input; Definition of Unique Fourier Series Coefficients	-2
Orientation of the Spatial Frequency Components	-5
IV. Input Data	IV-1
Technique for Discretizing Inputs	-1
Uniform Background and Contrast Changes	-1
V. Experiment	V-1
Plotting the $A(f_x, f_y)$ and $B(f_x, f_y)$ Coefficients	-1
Testing Methods	-4
Results	-4
VI. Conclusions and Recommendations	VI-1
Bibliography	BIB-1
Appendix A: Template Letters	A-1
Appendix B: Test Letters	B-1

List of Figures

<u>Figure</u>		<u>Page</u>
II-1	First Quadrant of the Modulation Transfer Function MTF(H) and MTF(L) of the Human Visual System . . .	II-2
III-1	Unique DFS Coefficients for an 8x8 Input	III-4
IV-1	Magnitudes of the DFT Coefficients of Letter A	IV-3
IV-2	Magnitudes of the DFT Coefficients of Letter A with Adjustment Factor Applied	IV-5
V-1	Quadrant I of Space 1	V-2
V-2	Quadrants of Space 2	V-3
V-3(a)	Coordinates and Clustering of Unfiltered Template Vectors in Space 1 .	V-5
V-3(b)	Coordinates and Clustering of Unfiltered Template Vectors in Space 2 .	V-6
V-3(c)	Coordinates and Clustering of MTF(H)- Filtered Template Vectors in Space 1 . .	V-7
V-3(d)	Coordinates and Clustering of MTF(H)- Filtered Template Vectors in Space 2 . .	V-8
V-3(e)	Coordinates and Clustering of MTF(L)- Filtered Template Vectors in Space 1 . .	V-9
V-3(f)	Coordinates and Clustering of MTF(L)- Filtered Template Vectors in Space 2 . .	V-10
V-4(a)	Test Results Using Unfiltered DFS Coefficients Plotted in Space 1	V-12
V-4(b)	Test Results Using Unfiltered DFS Coefficients Plotted in Space 2	V-13
V-4(c)	Test Results Using MTF(H)-Filtered DFS Coefficients Plotted in Space 1	V-14
V-4(d)	Test Results Using MTF(H)-Filtered DFS Coefficients Plotted in Space 2	V-15

List of Figures

<u>Figure</u>		<u>Page</u>
V-4(e)	Test Results Using MTF(L)-Filtered DFS Coefficients Plotted in Space 1	V-16
V-4(f)	Test Results Using MTF(L)-Filtered DFS Coefficients Plotted in Space 2	V-17
A-1	Gray Scale Used for Representation of Template Letters	A-1
A-2	Letters Used as Templates	A-2
B-1	Gray Scale Used for Representation of Test Letters	B-1
B-2	Letters Used as Test Inputs	B-2

Abstract

This research focused on representing the magnitude, phase, and orientation of each two-dimensional spatial frequency component of an input as a three-dimensional vector. An extension of the concept of phasor analysis was developed to facilitate this representation. Using Fourier analysis theory, any input can be considered as the sum of its spatial frequency components. Therefore, the input could be represented by a three-dimensional vector which was the summation of the vector representations of the spatial frequency components.

This theory was tested in two phases. First, isolated English capital letters A through Z were discretized using an 8x8 grid intended to simulate an input sensor device. The vectors representing these inputs were examined to insure that the letters were separable and letters which appeared as similar to human observers were clustered. Second, twenty test letters were used to test the capability of this scheme in recognizing variants of the templates. Each phase was tested using unfiltered spatial frequency components and components filtered by the modulation transfer function (MTF) of the human visual system, and the vectors were plotted in one of two spaces.

The template letters were separable and similar letters were clustered. The recognition rate ranged from 40% to 60%, depending on the choice of input filter and space used to plot the vectors.

I. Introduction

Many theories concerning the processing of information by the human visual system have been hypothesized in the past 20 years. One of these theories, based on psycho-physiological studies, is the size and orientation (spatial frequency) channel theory proposed by Campbell and Robson (Ref 6). In addition to this theory, the model developed by Kabrisky (Ref 11), which is based on anatomical studies of the visual cortex, proposed that the cortical-cortical connections between the primary and secondary visual cortex could support Fourier or similar transformation computations. This theory and model of the human visual system were the basis for many pattern recognition systems using spatial frequency analysis which have been developed in recent years.

Background

Much research has been done at the Air Force Institute of Technology, in conjunction with the Aerospace Medical Research Laboratory, and at other research centers trying to emulate the human visual system, based on the premise that the human visual system processes information and performs pattern recognition in the spatial frequency domain. This research focused on developing algorithms which computed correlations of low spatial frequency components of input data to identify English letters (Ref 20), the cyrillic alphabet and objects in reconnaissance photographs (Ref 22),

and Chinese characters (Ref 1). These efforts were successful, and they demonstrated that the low spatial frequency components contained the essence of the input form.

While these pattern recognition efforts were successful, much potentially valuable information was deleted when the high spatial frequency components were discarded. This information may be unnecessary for identifying a letter or an object, but it is essential for identifying the font of the letter or the detail of the object. But retaining this additional information required much additional storage space if a correlation of all of the spatial frequency components was required. Therefore, another method of retaining essential spatial frequency information is needed, since storage space is a prime consideration.

Problem

The objective of this study was to develop a method for representing the magnitude, phase, and orientation of each spatial frequency component of an input as a vector in three-dimensional space. A technique called phasor analysis, frequently used to represent the magnitude and phase of one-dimensional sinusoids as a two-dimensional vector, was extended to allow two-dimensional sinusoids to be represented. Using Fourier analysis theory, an input scene can be considered as the sum of its spatial frequency components. Once each spatial frequency component is represented as a single vector in three-dimensional space, then the entire

input scene can be represented by a vector sum, which is also a single vector in three-dimensional space.

Scope

The input data used as templates for this research were isolated English capital letters A through Z, handprinted of an 8x8 grid. The grid was intended to simulate an ideal 64-element sensor array, and each element was assumed to respond linearly to the radiance of the corresponding section of the input character. The letters were drawn to completely fill the grid, and were discretized by visually determining the extent that each element was filled by the character. Each element was divided into 8 subelements, and each subelement was assigned a nominal value of 1.0 (arbitrary units). If all subelements were filled, the element was assigned a value of 0, and if all subelements were empty, the element was assigned a value of 8.

In addition, uniform changes in background radiance and contrast were simulated. An adjustment factor was used to compensate for the effects of these changes on the Fourier Transform of the input.

General Approach

The template letters were discretized as discussed previously, and the unique Fourier Series coefficients (determined from the discrete Fourier Transform coefficients) of the spatial frequency components were computed. In

separate tests, the modulation transfer function (MTF) of the human visual system was applied to the coefficients to emulate the spatial frequency response of the visual system. In all tests, the three-dimensional vector sum representing each template was determined in two different spaces, denoted Space 1 and Space 2. As part of the experiment, the template vectors were examined to insure the letters were separable and letters that appear similar to human observers were clustered in these spaces.

The ability of this method to identify variants of the templates was also tested. Twenty test letters, which ranged from minor to extreme variants of the templates, were used for these tests.

Sequence of Presentation

Background on a current theory of human visual information processing that is based on the hypothesis that the visual system functions as a spatial frequency analyzer is provided in the next chapter. In chapter III, an overview of Fourier analysis theory, and a method for determining the orientation of spatial frequency components are presented. In chapter IV, the method used for inputting data and the problem of background radiance and contrast changes are discussed. In Chapter V, the experimental procedures, the results of the experiment, and the criteria used to evaluate the results are described. The conclusions based on this research and recommendations for future study are discussed in Chapter VI.

Discretized versions of the template letters used in this research are given in Appendix A. Discretized versions of the test letters are given in Appendix B.

II. The Human Visual System

Human Visual System as a Spatial Frequency Analyzer

One of the current theories of human visual information processing hypothesizes that the human visual system functions as a multi-channel spatial frequency analyzer. According to the theory proposed by Campbell and Robson (Ref 6), the human visual system is composed of many narrow bandwidth channels, each tuned to a different center frequency. The modulation transfer function, or contrast sensitivity of the human visual system as described by Ginsburg (Ref 8), is hypothesized to be the resultant of the combined activity of these individual channels. Studies by Glezer et al. (Ref 9) suggest that the receptive fields of the retina and the corresponding receptive fields of the primary visual cortex respond as narrow bandwidth spatial frequency filters such as those suggested by Campbell and Robson. Other studies by Maffei and Fiorentini (Ref 14,15), and Tootell et al. (Ref 23) suggest that the primary visual cortex may be organized as a spatial frequency analyzer, with spatial frequency and orientation information segmented within the substructure of the primary visual cortex.

These psychological and psycho-physiological experiments support the hypothesis that the visual system extracts contrast information, categorized according to spatial frequency and orientation, from the input scene. Exactly how spatial frequency and orientation information may be stored

or if this information is the basis for pattern recognition within the human brain remains a mystery.

Modulation Transfer Function of the Human Visual System

Since this research was attempting to emulate the human visual system as a spatial frequency analyzer, the modulation transfer function (MTF) as defined by Ginsburg (Ref 8) was used as a spatial frequency filter to simulate the spatial frequency response of the human visual system. In order to apply the MTF, the spatial frequencies f_x, f_y had to be defined in terms of cycles/degree. Therefore, the spatial frequency spectrum of the input image was defined as having a fundamental frequency of 1 cycle/degree, and the highest frequency present was 4 cycles/degree. Then, the MTF could be applied. Ginsburg used both an MTF(H) and an MTF(L), which were results of two different psycho-physiological experiments by Blakemore and Campbell (Ref 2), and Campbell, Kulikowski, and Levison (Ref 4), respectively. Therefore, both the MTF(H) and MTF(L) were used in this research. The first quadrants of the MTF(H) and MTF(L) in the range of 1 to 4 cycles/degree are shown in Figure II-1.

1	.79	.85	.90	.94
.77	.72	.78	.83	.87
.83	.77	.75	.77	.82
.87	.80	.75	.74	.78
.90	.84	.78	.77	.78

(a)MTF(H)

1	.23	.47	.60	.73
.19	.20	.42	.56	.68
.35	.34	.51	.64	.72
.54	.52	.59	.58	.69
.61	.60	.68	.67	.76

(b)MTF(L)

Figure II-1. First Quadrant of the Modulation Transfer Functions MTF(H) and MTF(L) of the Human Visual System (1 to 4 Cycles/Degree).(Ref 8:139-140).

III. Fourier Analysis

Overview of Fourier Analysis

In order to analyze the spatial frequency content of an input scene, the coefficients of the spatial frequency components of the scene must be determined. Digitally, this determination is made by computing the discrete Fourier transform (DFT), which is usually computed using a Fast Fourier Transform (FFT) algorithm. A detailed discussion of the DFT and the FFT can be found in the text by Oppenheim and Shafer (Ref 18). Only a brief overview will be presented here.

Since an infinite number of computations cannot be made, the continuous Fourier Transform of an input cannot, in general, be computed directly. Therefore, an approximation is used by computing the Fourier transform of discrete number of samples. This computation is known as the DFT. The FFT is simply a more efficient method of computing the DFT.

To compute the two-dimensional DFT, the input scene $f(x,y)$, which is of infinite extent, must be redefined as $f'(x,y)$, where $f'(x,y)$ is the product of the original $f(x,y)$ and a rectangular windowing function of dimension M samples by N samples. Therefore, the function $f'(x,y)$ is defined as:

$$\begin{aligned} f'(x,y) &= f(x,y) & (0 \leq x \leq M-1; 0 \leq y \leq N-1) \\ &= 0 & (\text{e.w.}) \end{aligned} \tag{1}$$

Now the discrete Fourier coefficients can be computed. The computations are made according to the following equations:

$$A(f_x, f_y) = \sum_y \sum_x f'(x, y) \cos(2\pi(f_x \cdot x + f_y \cdot y)) \quad (2a)$$

$$B(f_x, f_y) = \sum_y \sum_x f'(x, y) \sin(2\pi(f_x \cdot x + f_y \cdot y)) \quad (2b)$$

where $A(f_x, f_y)$ is the real part of the coefficient of spatial frequency component f_x, f_y ; and, $B(f_x, f_y)$ is the imaginary part of the coefficient of the spatial frequency component f_x, f_y . The scaling factor $1/M \cdot N$ was assumed to be part of the inverse Fourier transform; therefore, it was neglected here.

However, not all of these $A(f_x, f_y)$ and $B(f_x, f_y)$ coefficients are unique, since the DFT is a folded transform and the coefficients are present in conjugate pairs. For example, an 8×8 (64 sample) input has 34 unique $A(f_x, f_y)$ coefficients and 30 unique $B(f_x, f_y)$ coefficients, with the remaining coefficients being either always zero or conjugates of another coefficient.

DFT of a Two-Dimensional Input; Definition of Unique Fourier Series Coefficients

The DFT of a two-dimensional input requires the input to be multiplied, sample by sample, times a set of discretized two-dimensional basis functions of the general forms $\cos[2\pi(f_x \cdot x + f_y \cdot y)]$ and $\sin[2\pi(f_x \cdot x + f_y \cdot y)]$. In order for the

orientation of the particular basis function to be determined, the function must be in "fundamental" form, with $|fx| \leq M/2$ and $|fy| \leq N/2$. In compliance with the Nyquist criteria, $M/2, N/2$ is the maximum spatial frequency that can exist in an M sample by N sample input without aliasing.

When the DFT was computed using equations (2a) and (2b), the "fundamental" spatial frequencies were $K \leq fx \leq M/2$ and $L \leq fy \leq N/2$, where:

$$K = -M/2 + 1 \quad \text{for } M \text{ even;} \quad (3a)$$

$$K = -M/2 \quad \text{for } M \text{ odd;} \quad (3b)$$

$$L = -N/2 + 1 \quad \text{for } N \text{ even; and,} \quad (3c)$$

$$L = -N/2 \quad \text{for } N \text{ odd.} \quad (3d)$$

It is necessary to compute only the Fourier coefficients at spatial frequencies in the ranges $0 \leq fx \leq M/2$ and $L \leq fy \leq N/2$, since the remaining coefficients are the conjugates of these coefficients.

In terms of a discrete Fourier Series (DFS) representation of the input, each DFT coefficient and its conjugate are combined to yield a single coefficient of each sine and cosine component of the input. The DFS coefficients, which are defined as unique Fourier Series coefficients, of an 8×8 (64 sample) input are shown in Figure III-1. The factor of 2 accounts for the conjugate coefficient at the corresponding "negative" spatial frequency in a DFT representation.

A(0,0)	2A(1,1)	2A(3,2)	2A(1,-3)
2A(1,0)	2A(1,2)	2A(3,3)	2A(2,-1)
2A(2,0)	2A(1,3)	2A(3,4)	2A(2,-2)
2A(3,0)	2A(1,4)	2A(4,1)	2A(2,-3)
A(4,0)	2A(2,1)	2A(4,2)	2A(3,-1)
2A(0,1)	2A(2,2)	2A(4,3)	2A(3,-2)
2A(0,2)	2A(2,3)	A(4,4)	2A(3,-3)
2A(0,3)	2A(2,4)	2A(1,-1)	
A(0,4)	2A(3,1)	2A(1,-2)	
2B(1,0)	2B(1,3)	2B(3,3)	2B(2,-1)
2B(2,0)	2B(1,4)	2B(3,4)	2B(2,-2)
2B(3,0)	2B(2,1)	2B(4,1)	2B(2,-3)
2B(0,1)	2B(2,2)	2B(4,2)	2B(3,-1)
2B(0,2)	2B(2,3)	2B(4,3)	2B(3,-2)
2B(0,3)	2B(2,4)	2B(1,-1)	2B(3,-3)
2B(1,1)	2B(3,1)	2B(1,-2)	
2B(1,2)	2B(3,2)	2B(1,-3)	

Figure III-1. Unique DFS Coefficients for an 8x8 Input.

Orientation of the Spatial Frequency Components

The orientation of the spatial frequency components was determined by examining the lines of zero phase as outlined by Goodman (Ref 10:8-9). The lines of zero phase indicated the orientation of the particular basis function, i.e.

$\cos[2\pi(f_x \cdot x + f_y \cdot y)]$ and $\sin[2\pi(f_x \cdot x + f_y \cdot y)]$, in the x-y plane. The orientation angle θ with respect to the x-axis is given by:

$$\theta = \arctan (f_y / f_x) \quad (4)$$

where f_x and f_y are the "fundamental" spatial frequencies of the basis functions.

IV. Input Data

Technique for Discretizing Inputs

The input data used as templates for this experiment were handprinted English capital letters A through Z, drawn on an 8x8 grid. The grid was intended to ideally simulate a 64-element sensor array which may be used as an input device to a character recognition system. The sensor response was assumed to be linear with respect to the radiance of the input. The letters were drawn to completely fill the grid, and were discretized by subdividing each element of the grid into eight subelements and visually determining the extent that each subelement was filled by the character. Minor adjustments were made on the template letters during the discretizing process to maintain symmetry. If all of the subelements were filled, the element was given a value of 0. If all subelements were empty, the element was given a value of 8. Twenty test letters were discretized in the same manner. The template letters and test letters are shown in Appendix A and Appendix B, respectively.

Uniform Background and Contrast Changes

Since this was an attempt to simulate a sensor array input device, uniform changes in contrast and background radiance were also simulated. Changes in background radiance were simulated by adjusting the value of each subelement

within the elements of the grid. If the background radiance was increased by 50%, then each subelement was assigned the value 1.5. Therefore, if all of the subelements were filled, the value remained 0, but if all subelements were empty, the value increased to 12.

The contrast of an image is defined by:

$$C = L_{\max} - L_{\min} / L_{\max} + L_{\min} \quad (6)$$

where L_{\max} and L_{\min} are the maximum and minimum radiances, respectively. The contrast remains constant for changes in background radiance. Uniform contrast changes were simulated by adding a constant to the value of each element of the grid. While uniform changes in the contrast had no effect on the value of the DFT coefficients (other than changing the value of the 0,0; or d.c. term), background changes had a definite effect on the value of the coefficients. The effects of uniform changes in background radiance and contrast on the DFT coefficients for the letter A are shown in Figure IV-1.

4.79	17.85	11.55	45.67	11.55	17.85	4.79	0.00
5.62	17.89	51.54	40.79	51.54	17.89	5.62	0.00
17.73	43.10	42.81	47.61	42.81	43.10	17.73	0.00
18.37	22.63	44.35	288.00	44.35	22.63	18.37	0.00
17.73	43.10	42.81	47.61	42.81	43.10	17.73	0.00
5.62	17.89	51.54	40.79	51.54	17.89	5.62	0.00
4.79	17.85	11.55	45.67	11.55	17.85	4.79	0.00
12.25	11.31	29.56	48.00	29.56	11.31	12.25	0.00

a) Letter A with Lmax = 8 and Lmin = 0

7.18	26.78	17.33	68.50	17.33	26.78	7.18	0.00
8.43	26.83	77.31	61.19	77.31	26.83	8.43	0.00
26.60	64.65	64.22	71.41	64.22	64.65	26.60	0.00
27.55	33.94	66.52	432.00	66.52	33.94	27.55	0.00
26.60	64.65	64.22	71.41	64.22	64.65	26.60	0.00
8.43	26.83	77.31	61.19	77.31	26.83	8.43	0.00
7.18	26.78	17.33	68.50	17.33	26.78	7.18	0.00
18.37	16.97	44.35	72.00	44.35	16.97	18.37	0.00

b) Letter A with Lmax = 12 and Lmin = 0

4.79	17.85	11.55	45.67	11.55	17.85	4.79	0.00
5.62	17.89	51.54	40.79	51.54	17.89	5.62	0.00
17.73	43.10	42.81	47.61	42.81	43.10	17.73	0.00
18.37	22.63	44.35	544.00	44.35	22.63	18.37	0.00
17.73	43.10	42.81	47.61	42.81	43.10	17.73	0.00
5.62	17.89	51.54	40.79	51.54	17.89	5.62	0.00
4.79	17.85	11.55	45.67	11.55	17.85	4.79	0.00
12.25	11.31	29.56	48.00	29.56	11.31	12.25	0.00

c) Letter A with Lmax = 12 and Lmin = 4

Figure IV-1. Magnitudes of the DFT Coefficients of Letter A.

Since it is desirable for a system to be independent of changes in background radiance and contrast, an adjustment factor was necessary. This adjustment factor F was determined to be:

$$F = (A(0,0)/M \cdot N) - L_{min} \quad (7)$$

where $A(0,0)/M \cdot N$ is the d.c. component, or average radiance of the input, and L_{min} is the minimum radiance of the input.

When each spatial frequency component is divided by this adjustment factor, the DFT becomes independent of uniform changes in background radiance and contrast. The results of using the adjustment factor F on the DFT coefficients of the letter A are shown in Figure IV-2.

This adjustment factor was very effective in eliminating adverse effects due to uniform background luminance and contrast changes. The adjusted DFT coefficients were found to remain precise to two decimal places for uniform changes in the values of background luminance (L_{max}) ranging from 0.04 to 80,000; and for uniform contrast changes ranging from 1 (maximum contrast) to 0.04. The errors at the limits were attributable to rounding errors in the sine and cosine basis functions used for computation of the DFT coefficients.

1.06	3.97	2.57	10.15	2.57	3.97	1.06	0.00
1.25	3.98	11.45	9.06	11.45	3.98	1.25	0.00
3.94	9.58	9.51	10.58	9.51	9.58	3.94	0.00
4.08	5.03	9.85	64.00	9.85	5.03	4.08	0.00
3.94	9.58	9.51	10.58	9.51	9.58	3.94	0.00
1.25	3.98	11.45	9.06	11.45	3.98	1.25	0.00
1.06	3.97	2.57	10.15	2.57	3.97	1.06	0.00
2.72	2.51	6.57	10.67	6.57	2.51	2.72	0.00

a) Letter A with $L_{max} = 8$ and $L_{min} = 0$

1.06	3.97	2.57	10.15	2.57	3.97	1.06	0.00
1.25	3.98	11.45	9.06	11.45	3.98	1.25	0.00
3.94	9.58	9.51	10.58	9.51	9.58	3.94	0.00
4.08	5.03	9.85	64.00	9.85	5.03	4.08	0.00
3.94	9.58	9.51	10.58	9.51	9.58	3.94	0.00
1.25	3.98	11.45	9.06	11.45	3.98	1.25	0.00
1.06	3.97	2.57	10.15	2.57	3.97	1.06	0.00
2.72	2.51	6.57	10.67	6.57	2.51	2.72	0.00

b) Letter A with $L_{max} = 12$ and $L_{min} = 0$

1.06	3.97	2.57	10.15	2.57	3.97	1.06	0.00
1.25	3.98	11.45	9.06	11.45	3.98	1.25	0.00
3.94	9.58	9.51	10.58	9.51	9.58	3.94	0.00
4.08	5.03	9.85	120.89	9.85	5.03	4.08	0.00
3.94	9.58	9.51	10.58	9.51	9.58	3.94	0.00
1.25	3.98	11.45	9.06	11.45	3.98	1.25	0.00
1.06	3.97	2.57	10.15	2.57	3.97	1.06	0.00
2.72	2.51	6.57	10.67	6.57	2.51	2.72	0.00

c) Letter A with $L_{max} = 12$ and $L_{min} = 4$

Figure IV-2. Magnitudes of the DFT Coefficients of Letter A with Adjustment Factor Applied.

V. Experiment

Plotting the $A(f_x, f_y)$ and $B(f_x, f_y)$ Coefficients

Sinusoids are often represented as vectors in the complex number plane in a technique known as phasor analysis. In phasor analysis, the coefficient of a sinusoid is plotted as a vector of given magnitude and phase. Representing sinusoids in this manner reduces the addition and subtraction of sinusoids to simple algebraic manipulations of complex numbers.

Since the unique Fourier Series coefficients as defined previously are coefficients of sinusoids, they can be used to represent the spatial frequency component as a vector. The complex plane used to plot the magnitude and phase of each two-dimensional Fourier Series coefficients was oriented at the orientation angle θ equivalent to the orientation of the basis function of the coefficient being plotted. Two complex spaces, designated Space 1 and Space 2, were used to plot the two-dimensional Fourier Series coefficients as three-dimensional phasors.

In Space 1, the unique $A(f_x, f_y)$ coefficient was plotted in the x-y plane at an angle θ , equal to the orientation angle, from the x-axis. The corresponding $B(f_x, f_y)$ coefficient was plotted in the +z direction, orthogonal to the $A(f_x, f_y)$ coefficient. This yielded a single vector, $\{A(f_x, f_y)\cos \theta, A(f_x, f_y)\sin \theta, B(f_x, f_y)\}$, which represented the component at two-dimensional spatial frequency f_x, f_y . The

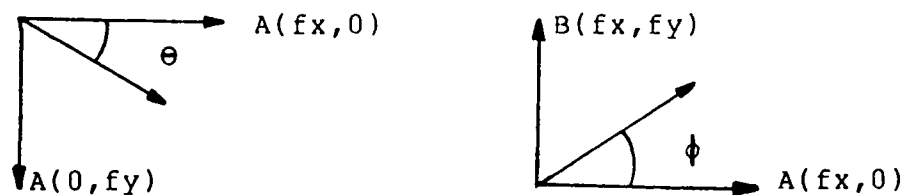
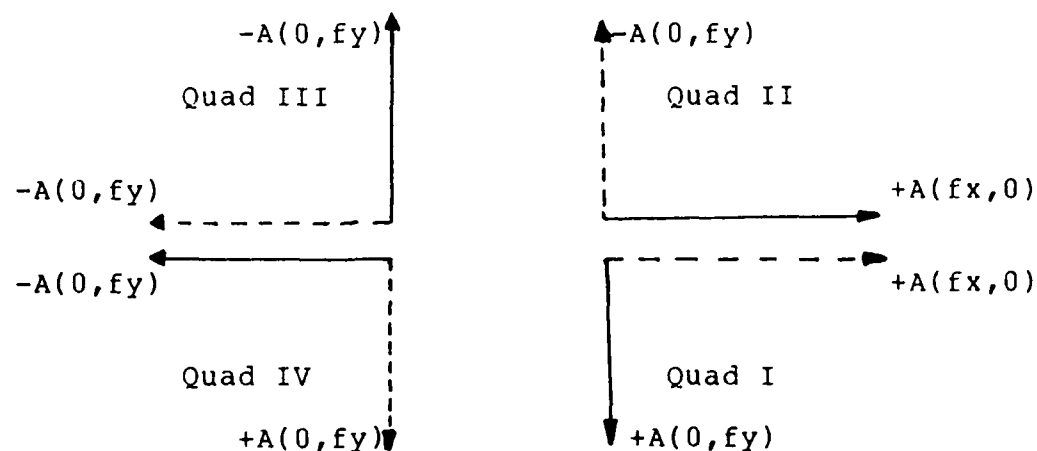


Figure V-1. Quadrant I of Space 1.

input scene $f'(x,y)$ was represented by a vector sum of its unique spatial frequency components. A pictorial representation of Quadrant I of Space 1 is given in Figure V-1.

In space 2, the coefficients were plotted differently. A coefficient and its conjugate, computed using the DFT, at a particular spatial frequency pair fx, fy and $-fx, -fy$, respectively, were plotted such that they summed vectorally, to yield the unique Fourier Series coefficient defined previously. For this to be accomplished, each quadrant of the space, which corresponded with a quadrant of the DFT, was defined differently. The quadrants of Space 2 are pictured in Figure V-2.



$+B(fx, fy)$ in $+z$ direction in Quadrants I and IV
 $-B(fx, fy)$ in $+z$ direction in Quadrants II and III

Figure V-2. Quadrants of Space 2.

In quadrant I, the positive $A(fx, fy; fx \geq 0, fy > 0)$ coefficients were plotted radially outward, and the positive $B(fx, fy; fx \geq 0, fy > 0)$ were plotted in the $+z$ direction. In quadrant II, the positive $A(fx, fy; fx > 0, fy \leq 0)$ were plotted radially outward, and the positive $B(fx, fy; fx > 0, fy \leq 0)$ coefficients were plotted in the $-z$ direction. In quadrant III, the positive $A(fx, fy; fx \leq 0, fy < 0)$ coefficients were plotted radially inward, and the $B(fx, fy; fx \leq 0, fy < 0)$ coefficients were plotted in the $-z$ direction. In quadrant IV, the positive $A(fx, fy; fx < 0, fy \geq 0)$ coefficients were plotted radially inward, and the positive $B(fx, fy; fx < 0, fy \geq 0)$ coefficients were plotted in the $+z$ direction.

Testing Methods

The hypothesis that the essential spatial frequency information can be retained in three-dimensional space was tested in two phases. In the first phase, six sets of templates were computed using discretized capital English letters A through Z. The template vector sets were computed using the unfiltered Fourier Series coefficients plotted in Space 1 and Space 2, the Fourier Series coefficients filtered by MTF(H) and plotted in Space 1 and Space 2, and the Fourier Series coefficients filtered by MTF(L) and plotted in Space 1 and Space 2. The template vector sets were examined to see that 1) the letters were separable in three-dimensional space; and 2) letters which human observers perceive as similar were clustered together.

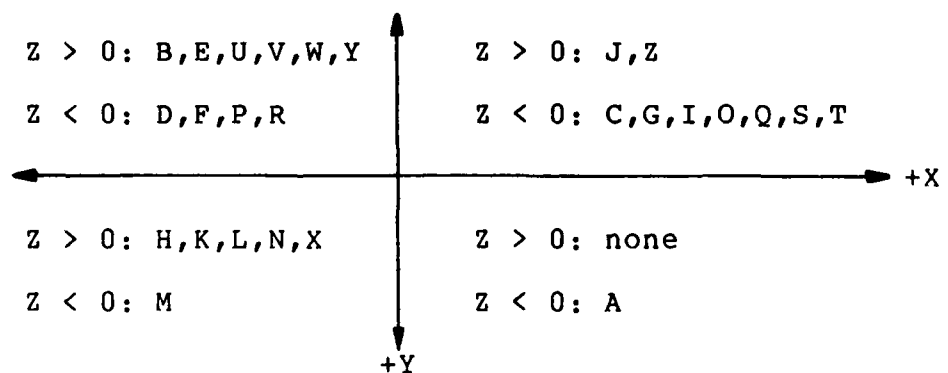
In the second phase, twenty test letter vectors were computed using methods corresponding to stored template vectors. The test letter vectors were then compared to the stored template vectors, using Euclidean distance as a metric.

Results

The template vectors for the handprinted English letters are given in Figures V-3(a)-(f). The letters were separable in this scheme, and the letters which looked most alike to human observers (C, G, O, and Q; P and R; H and N) were clustered together in all template sets.

<u>Letter</u>	<u>X</u>	<u>Y</u>	<u>Z</u>
A	8.58	59.85	-24.53
B	-32.24	-93.71	17.24
C	34.44	-50.94	-15.62
D	-37.97	-86.02	-40.52
E	-15.39	-50.81	48.79
F	-22.53	-43.56	0
G	37.24	-47.80	-14.20
H	-72.83	18.13	58.86
I	63.29	-59.63	-27.27
J	18.32	-15.61	86.47
K	-57.43	24.72	63.90
L	-64.39	0.60	37.84
M	-27.76	3.90	-43.46
N	-65.37	48.39	47.51
O	35.93	-45.45	-17.17
P	-33.48	-64.03	-25.76
Q	41.96	-22.36	-11.95
R	-32.75	-42.18	- 8.76
S	41.20	-43.17	-21.57
T	10.46	-66.42	- 1.71
U	-52.26	-34.18	79.57
V	-40.58	-17.68	30.15
W	-58.94	-25.88	84.73
X	-48.73	32.78	27.22
Y	-25.75	- 8.78	8.78
Z	2.37	-92.32	49.84

a) Coordinates

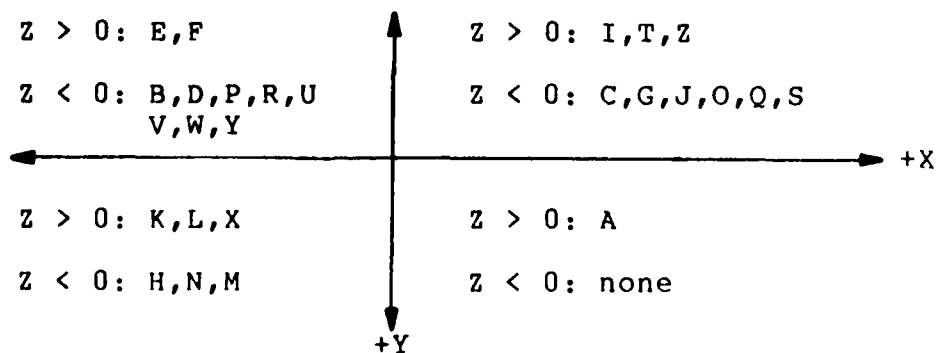


b) Clustering by Sectors

Figure V-3(a). Coordinates and Clustering of Unfiltered Template Vectors in Space 1.

<u>Letter</u>	<u>X</u>	<u>Y</u>	<u>Z</u>
A	8.58	41.90	46.47
B	-32.24	-105.17	-34.26
C	34.44	-50.65	-26.04
D	-37.97	-86.50	-17.51
E	-15.39	-64.00	17.66
F	-22.53	-62.99	8.05
G	37.24	-46.22	-35.37
H	-72.83	9.14	-51.50
I	63.29	-59.84	20.47
J	18.32	-14.48	-30.62
K	-57.43	21.37	3.97
L	-64.39	8.22	6.31
M	-27.76	0.26	-48.16
N	-65.37	38.10	-66.13
O	35.93	-44.07	-59.13
P	-33.48	-82.99	-25.62
Q	41.96	-18.42	-70.51
R	-32.75	-62.21	-37.20
S	41.20	-44.73	-36.45
T	10.46	-63.47	6.30
U	-52.26	-21.81	-94.22
V	-40.58	-9.92	-38.20
W	-58.94	-12.40	-104.90
X	-48.73	32.78	41.45
Y	-25.75	-3.06	-21.54
Z	2.37	-81.14	74.31

a) Coordinates

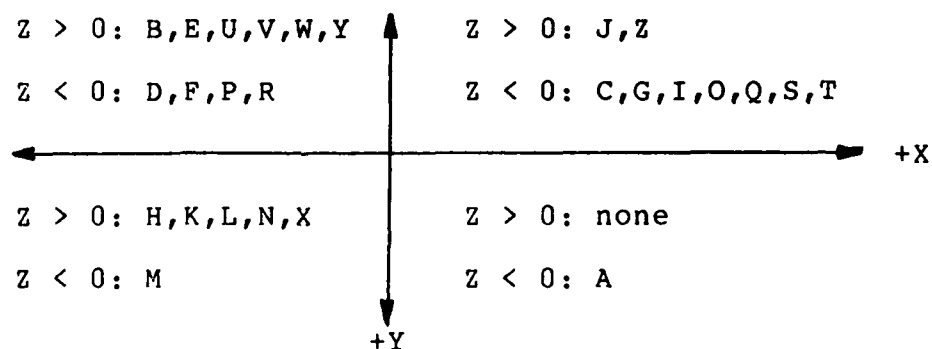


b) Clustering by Sectors

Figure V-3(b). Coordinates and Clustering of Unfiltered Template Vectors in Space 2.

<u>Letter</u>	<u>X</u>	<u>Y</u>	<u>Z</u>
A	4.46	46.71	-17.18
B	-29.72	-73.87	18.35
C	24.30	-39.84	-12.59
D	-35.97	-67.48	-28.55
E	-16.79	-41.11	39.07
F	-22.74	-37.73	- 0.98
G	26.50	-37.69	-11.05
H	-59.09	13.88	49.22
I	49.36	-46.74	-20.79
J	15.87	-11.28	70.70
K	-50.35	17.98	46.10
L	-55.04	2.77	31.19
M	-24.49	2.43	-30.58
N	-51.98	36.14	39.89
O	25.50	-36.02	-11.19
P	-30.66	-53.28	-18.19
Q	31.11	-18.70	- 6.89
R	-30.23	-37.09	- 5.82
S	31.43	-34.26	-16.99
T	7.91	-55.43	- 1.54
U	-43.16	-26.19	65.00
V	-30.58	-13.54	21.53
W	-47.86	-19.89	67.96
X	-34.18	24.60	17.56
Y	-18.29	- 7.35	5.01
Z	1.85	-72.81	39.00

a) Coordinates

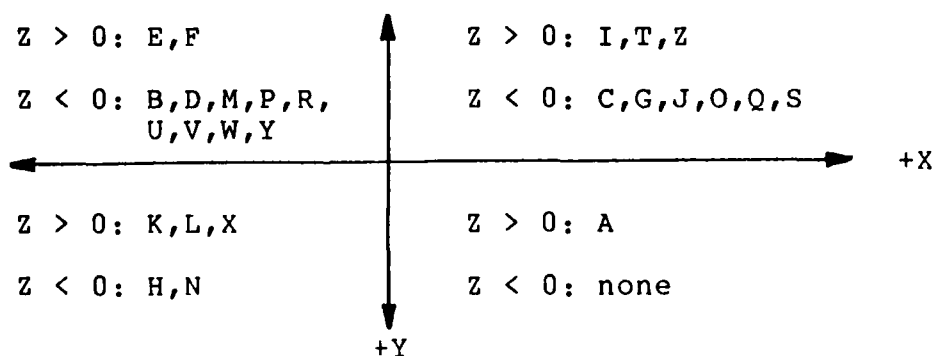


b) Clustering by Sectors

Figure V-3(c). Coordinates and Clustering of MTF(H)-Filtered Template Vectors in Space 1.

<u>Letter</u>	<u>X</u>	<u>Y</u>	<u>Z</u>
A	4.46	32.04	33.76
B	-29.72	-83.23	-25.32
C	24.30	-39.78	-19.27
D	-35.97	-67.86	-12.00
E	-16.79	-51.72	17.16
F	-22.74	-53.26	6.49
G	26.50	-36.57	-26.69
H	-59.09	6.58	-43.63
I	49.36	-46.90	19.28
J	15.87	-10.05	-25.14
K	-50.35	15.25	3.10
L	-55.04	8.80	7.35
M	-24.49	- 0.35	-43.11
N	-51.98	28.13	-53.91
O	25.50	-34.95	-45.95
P	-30.66	-68.66	-20.10
Q	31.11	-15.60	-54.25
R	-30.23	-53.30	-27.31
S	31.43	-35.65	-27.22
T	7.91	-52.90	5.16
U	-43.16	-15.95	-74.67
V	-30.58	- 7.18	-27.01
W	-47.86	- 8.92	-82.99
X	-34.18	24.60	29.86
Y	-18.29	- 2.64	-16.42
Z	1.85	-64.12	58.95

a) Coordinates

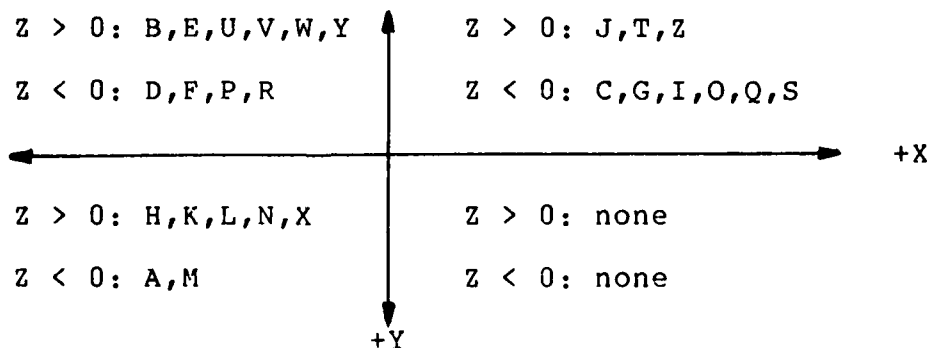


b) Clustering by Sectors

Figure V-3(d). Coordinates and Clustering of MTF(H)-Filtered Template Vectors in Space 2.

<u>Letter</u>	<u>X</u>	<u>Y</u>	<u>Z</u>
A	- 0.13	25.68	- 3.10
B	-15.53	-33.47	0.30
C	10.47	-14.98	- 8.28
D	-23.07	-26.83	-18.20
E	- 5.42	-10.02	13.79
F	- 6.93	-13.29	- 0.80
G	11.59	-14.93	- 7.54
H	-24.53	7.05	24.58
I	20.99	-20.92	-14.56
J	12.44	- 3.39	39.35
K	-25.36	9.26	15.08
L	-32.63	4.43	11.43
M	- 3.87	5.55	-20.67
N	-17.43	17.64	22.74
O	11.37	-11.90	5.69
P	-12.02	-22.85	-12.30
Q	14.52	- 2.85	- 9.72
R	-12.48	-16.60	-14.35
S	15.20	-13.87	-10.93
T	0.68	-26.56	0.26
U	-22.98	-13.87	36.10
V	-13.89	- 8.77	14.71
W	-25.52	-14.76	36.26
X	-11.42	13.68	7.19
Y	- 9.12	- 2.42	6.67
Z	1.03	-29.40	11.27

a) Coordinates

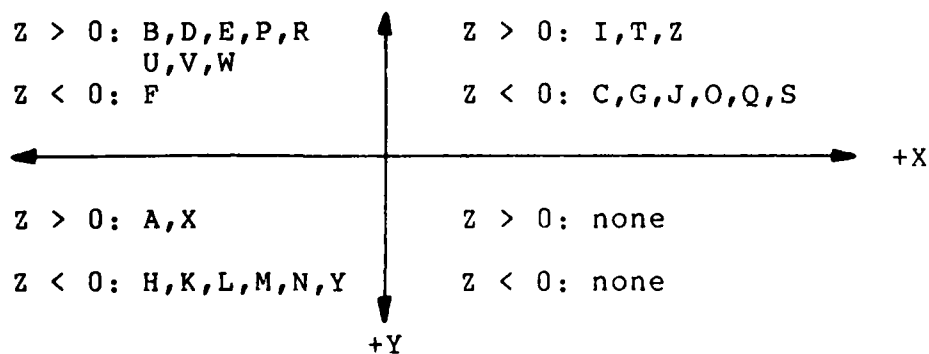


b) Clustering by Sectors

Figure V-3(e). Coordinates and Clustering of MTF(L)-Filtered Template Vectors in Space 1.

<u>Letter</u>	<u>X</u>	<u>Y</u>	<u>Z</u>
A	- 0.13	14.49	19.12
B	-15.53	-40.45	-15.94
C	10.47	-14.82	- 9.62
D	-23.07	-27.32	- 2.96
E	- 5.42	-18.62	- 0.58
F	- 6.93	-25.96	2.29
G	11.59	13.88	-12.52
H	-24.53	1.37	-22.55
I	20.99	-21.05	3.91
J	12.44	3.17	-13.92
K	-25.36	6.97	- 2.30
L	-32.63	9.40	- 2.55
M	- 3.87	3.16	-18.79
N	-17.43	10.86	-26.04
O	11.37	-11.01	-21.49
P	-12.02	-34.87	- 4.78
Q	14.52	- 0.26	-27.24
R	-12.48	-29.31	- 8.44
S	15.20	-14.59	-12.90
T	0.68	-24.91	1.62
U	-22.98	6.34	-39.14
V	-13.89	- 3.95	- 5.86
W	-25.52	- 6.37	-44.57
X	-11.42	13.68	14.16
Y	- 9.12	1.10	- 2.75
Z	1.03	-21.85	23.31

a) Coordinates



b) Clustering by Sectors

Figure V-3(f). Coordinates and Clustering of MTF(L)-Filtered Template Vectors in Space 2.

Next, the test letter vectors were compared with the stored template vectors. The results of these test are given in Figures V-4(a)-(f). The criteria used to determine the best results involved looking for not only the scheme with the most correct identifications of the test letters, but also looking for the scheme with the lowest rank total (sum of the positions 1-26 of the correct identity of the test letters). In addition, the number of times the correct identity of the letter was first or second alternative was examined. This may be useful if this character recognition technique was used in conjunction with a tree-organized word recognizer.

The best results were achieved using no filtering and plotting the coefficients in Space 2. Using this scheme, 60% recognition was achieved (75% of the letters were at least the second alternative), and most of the substitutions made appeared to be reasonable substitutions (Y for H; F for P; Z for I; J for O; C for G). Only two of the substitutions, O for T and X for L did not appear to be reasonable substitutions. The remaining methods achieved 40% to 55% recognition.

<u>Test Letter</u>	<u>Identity</u>	<u>Distance</u>	<u>Ranking</u>	<u>Distance to Correct Identity</u>
A	A	16.51	1	-----
A	A	11.68	1	-----
A	A	31.73	1	-----
H, A*	M	32.49	2(A)	43.00
H	X	17.45	7	54.32
T	C	46.01	5	49.85
P	M	52.48	2	84.73
I	G	27.29	11	58.29
X	X	24.18	1	-----
H	H	29.73	1	-----
L	X	50.36	4	68.97
C	Q	13.85	5	22.22
O	Q	30.44	3	39.62
G	Q	38.26	2	42.31
N	X	17.28	5	44.75
K	K	9.06	1	-----
N	N	9.31	1	-----
A	A	23.84	1	-----
Z	Z	15.23	1	-----
H	L	36.92	4	54.91

Total Number Correct: 9

Total Number Ranked
One, Two, or Three: 13

Total Ranking Score: 59

* This letter was identified as either H or A by human
observers; ranking was based on position of either H or A.

Figure V-4(a). Test Results Using Unfiltered DFS Coefficients
Plotted in Space 1.

<u>Test Letter</u>	<u>Identity</u>	<u>Distance</u>	<u>Ranking</u>	<u>Distance to Correct Identity</u>
A	A	6.47	1	-----
A	A	15.66	1	-----
A	A	39.69	1	-----
H, A*	Y	25.16	7(H)	67.23
H	H	30.61	1	-----
T	O	35.07	10	66.40
P	F	38.07	10	72.24
I	Z	42.32	4	60.59
X	X	20.07	1	-----
H	H	27.84	1	-----
L	X	26.57	3	57.81
C	C	33.29	1	-----
O	J	24.73	4	50.93
G	C	25.47	3	29.16
N	H	23.52	2	27.17
K	K	4.23	1	-----
N	N	6.81	1	-----
A	A	18.66	1	-----
Z	Z	10.30	1	-----
H	H	13.86	1	-----

Total Number Correct: 12

Total Number Ranked
One, Two, or Three: 15

Total Ranking Score: 55

* This letter was identified as either H or A by human
observers; ranking was based on position of either H or A.

Figure V-4(b). Test Results Using Unfiltered DFS Coefficients
Plotted in Space 2.

<u>Test Letter</u>	<u>Identity</u>	<u>Distance</u>	<u>Ranking</u>	<u>Distance to Correct Identity</u>
A	A	12.70	1	-----
A	A	10.23	1	-----
A	A	25.59	1	-----
H, A*	M	26.24	2(A)	33.39
H	X	10.65	8	43.55
T	C	36.95	5	41.34
P	M	46.67	2	70.92
I	O	19.26	10	46.18
X	X	16.65	1	-----
H	L	20.81	4	25.51
L	X	42.45	4	57.25
C	Q	7.02	4	18.34
O	Q	22.33	2	30.21
G	Q	29.28	3	34.18
N	X	13.09	5	32.50
K	K	6.46	1	-----
N	N	7.03	1	-----
A	A	18.18	1	-----
Z	Z	14.86	1	-----
H	L	28.98	5	46.74

Total Number Correct: 8

Total Number Ranked
One, Two, or Three: 12

Total Ranking Score: 62

* This letter was identified as either H or A by human
observers; ranking was based on position of either H or A.

Figure V-4(c). Test Results Using MTF(H)-Filtered DFS
Coefficients Plotted in Space 1.

<u>Test Letter</u>	<u>Identity</u>	<u>Distance</u>	<u>Ranking</u>	<u>Distance to Correct Identity</u>
A	A	4.66	1	-----
A	A	11.06	1	-----
A	A	29.20	1	-----
H, A*	Y	18.47	8 (H)	50.92
H	V	23.56	2	24.99
T	O	26.24	10	53.61
P	E	30.90	11	59.06
I	Z	33.50	4	46.99
X	X	13.22	1	-----
H	H	22.38	1	-----
L	X	30.48	2	46.82
C	J	27.38	2	27.48
O	J	19.90	5	39.71
G	C	19.43	3	23.06
N	H	18.01	2	18.81
K	K	3.21	1	-----
N	N	5.02	1	-----
A	A	14.16	1	-----
Z	Z	6.64	1	-----
H	H	8.40	1	-----

Total Number Correct: 10

Total Number Ranked
One, Two, or Three: 15

Total Ranking Score: 58

* This letter was identified as either H or A by human
observers; ranking was based on position of either H or A.

Figure V-4(d). Test Results Using MTF(H)-Filtered DFS
Coefficients Plotted in Space 2.

<u>Test Letter</u>	<u>Identity</u>	<u>Distance</u>	<u>Ranking</u>	<u>Distance to Correct Identity</u>
A	A	6.24	1	-----
A	A	13.58	1	-----
A	M	22.25	2	24.89
H, A*	M	16.95	2(A)	29.45
H	X	8.39	11	29.13
T	C	13.84	7	19.67
P	M	20.73	3	35.90
I	F	10.31	16	28.88
X	X	9.90	1	-----
H	K	9.59	5	17.75
L	M	27.71	4	37.39
C	O	7.94	4	11.86
O	O	14.00	1	-----
G	O	18.15	3	20.54
N	Y	8.50	8	23.11
K	K	2.97	1	-----
N	N	3.60	1	-----
A	A	7.35	1	-----
Z	Z	11.88	1	-----
H	L	19.37	10	30.87

Total Number Correct: 8

Total Number Ranked
One, Two, or Three: 12

Total Ranking Score: 83

* This letter was identified as either H or A by human
observers; ranking was based on position of either H or A.

Figure V-4(e). Test Results Using MTF(L)-Filtered DFS
Coefficients Plotted in Space 1.

<u>Test Letter</u>	<u>Identity</u>	<u>Distance</u>	<u>Ranking</u>	<u>Distance to Correct Identity</u>
A	A	1.84	1	-----
A	A	9.13	1	-----
A	A	9.59	1	-----
H, A*	Y	14.11	2(A)	19.77
H	Y	9.81	6	18.12
T	O	13.16	7	22.89
P	Y	19.39	12	32.76
I	Z	14.80	8	26.58
X	X	5.13	1	-----
H	K	8.07	4	14.67
L	X	17.92	2	23.18
C	J	14.07	2	16.08
O	C	14.88	9	24.46
G	C	10.62	2	12.68
N	N	9.26	1	-----
K	K	2.51	1	-----
N	N	3.17	1	-----
A	A	10.77	1	-----
Z	Z	7.03	1	-----
H	H	4.82	1	-----

Total Number Correct: 10

Total Number Ranked
One, Two, or Three: 14

Total Ranking Score: 64

* This letter was identified as either H or A by human
observers; ranking was based on position of either H or A.

Figure V-4(f). Test Results Using MTF(L)-Filtered DFS
Coefficients Plotted in Space 2.

VI. Conclusions and Recommendations

This research exhibited a method to represent the spatial frequency content of an input as a three-dimensional vector representing the summation of the magnitude, phase, and orientation of the components. This vector was composed of the form of the input, contained in the low spatial frequency components, and the detail of the input, contained in the high spatial frequency components. Since only three dimensions were required to describe any input, templates could be stored efficiently, and distance computations were very simple. In contrast, other methods of pattern recognition utilizing spatial frequency components required the storage and correlation of 49 Fourier components and sacrificed the detail of the input by discarding the high spatial frequency components.

This research, while showing that phasor analysis in three-dimensions was possible, did have five definite shortcomings. First, the spatial frequency spectrum of the input was severely bandlimited, due the low spatial resolution associated with the simulated input sensor. In the human visual system, the spatial frequency spectrum of an input ranges from approximately 0.2 cycles/degree to approximately 50 cycles/degree, based on the filtering properties (MTF) of the system. In this research, the spatial frequency spectrum ranged from 1 cycle/degree to 4 cycles/degree. Even with this severe bandlimiting,

60 percent recognition was achieved. A higher resolution input technique should significantly improve the recognition rate. Second, pure sine and cosine inputs of differing spatial frequencies but of the same magnitude and orientation had identical vector representations when the components were unfiltered. Filtering of the spatial frequencies components using $MTF(H)$ and $MTF(L)$ did alleviate this problem, since each component was scaled differently. Another solution may be to use trigonometric identities to allow the spatial frequency components to be redefined in terms of the fundamental spatial frequencies. Third, only 26 template letters were used in this research. In the human visual system, hundreds of templates, or sets of template areas exist for the characters used as templates in this research. By employing more templates, statistical analysis could be used for pattern recognition. Fourth, noise effects were neglected. It is suspected that if the MTF of the human visual system is used, the noise performance of the vector-based system would be comparable to that of the human visual system. Finally, the effects of size variance were not examined. These are areas on which future research should be focused.

The concept of phasor representation of sinusoids and its applications to represent the spatial frequency content of an input appears to be a viable technique to reduce the dimensionality required to describe an input. Further research is necessary to determine the full impact of this technique in the area of pattern recognition.

Bibliography

1. Ankeney, L.A. The Classification of Chinese Characters by Spatial Filtering. Air Force Institute of Technology M.S. Thesis. GE/EE/67A-11, 1967.
2. Blakemore, C. and Campbell, F.W. "On the Existence of Neurons in the Human Visual System Selectively Sensitive to the Orientation and Size of Retinal Images," Journal of Physiology, 203: 237-260, 1969.
3. Campbell, F.W. and Kulikowski, J.J. "Orientation Selectivity of the Human Visual System," Journal of Physiology, 187: 437-445, 1966.
4. Campbell, F.W., Kulikowski, J.J., and Levison, J.Z. "The Effect of Orientation on the Visual Resolution of Gratings," Journal of Physiology, 187: 427-436, 1966.
5. Campbell, F.W. and Maffei, L. "Electrophysiological Evidence for the Existence of Orientation and Size Detectors in the Human Visual System," Journal of Physiology, 207: 635-652, 1970.
6. Campbell, F.W. and Robson, J.G. "Application of Fourier Analysis to the Visibility of Gratings," Journal of Physiology, 197: 551-566, 1968.
7. Ginsburg, A.P. Psychological Correlates of a Model of the Human Visual System. Air Force Institute of Technology M.S. Thesis. GE/EE/71S-2, 1971.
8. Ginsburg, A.P. Visual Information Processing Based on Spatial Filters Constrained by Biological Data. AMRL Technical Report TR-78-129 Vol. I and II. Wright-Patterson AFB, Ohio: Aerospace Medical Research Laboratory, 1978
9. Glezer, V.D., Ivanov, V.A., and Tscherbach, T.A. "Investigation of Complex and Hypercomplex Receptive Fields of Visual Cortex of the Cat as Spatial Frequency Filters," Vision Research, 13: 1875-1904, 1973.
10. Goodman, J.W. Introduction to Fourier Optics. San Francisco: McGraw-Hill Book Company, 1968.
11. Kabrisky, M. A Proposed Model for Visual Information Processing in the Human Brain. Urbana: University of Illinois Press, 1966

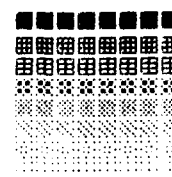
12. Kabrisky, M. "An Introduction to a Model of the Human Visual System," Proceedings of the National Aerospace Electronics Conference. 297-303. Dayton, Ohio: Dayton Section, IEEE, May 1973.
13. Klein, M.V. Optics. New York: John Wiley and Sons, 1970.
14. Maffei, L. and Fiorentini, A. "The Visual Cortex as a Spatial Frequency Analyser," Vision Research, 13: 1255-1267, 1973.
15. Maffei, L. and Fiorentini, A. "Spatial Frequency Rows in the Striate Visual Cortex," Vision Research, 17: 257-264, 1977.
16. Mostafavi, H. and Sakrison, D. "Structure and Properties of a Single Channel in the Human Visual System," Vision Research, 16: 957-968, 1976.
17. Movshon, J.A. and Blakemore, C.B. "Orientational Specificity and Spatial Selectivity in Human Vision," Perception, 2: 53-60, 1973.
18. Oppenheim, A.V. and Shafer, R.W. Digital Signal Processing. Englewood Cliffs: Prentice-Hall, 1975.
19. Polynak, S.L. The Vertebrate Visual System. Chicago: University of Chicago Press, 1957.
20. Radoy, C.H. Pattern Recognition by Fourier Series Transformation. Air Force Institute of Technology M.S. Thesis. GE/EE/67A-11, 1967.
21. Sachs, M., Nachmias, J., and Robson, J.G. "Spatial Frequency Channels in Human Vision," J. Opt. Soc. Am., 61: 1176-1186, 1971.
22. Tootell, R.B., Silverman, M.S., and DeValois, R.L. "Spatial Frequency Columns in Primary Visual Cortex," Science, 214: 813-815, 1981.
23. Watanabe, A., Mori, T., Nagata, S., and Hiwatashi, K. "Spatial Sine-wave Response of the Human Visual System," Vision Research, 8: 1245-1263, 1968.

APPENDIX A

The template letters used in this research are shown in numerical and gray scale representation in Figure A-2. The gray scale used for the representations is given in Figure A-1, and ranges from 0 (black) to 8 (white). To observe the representations with the fundamental spatial frequency equal to 1 cycle/degree, the letters should be viewed at a distance of approximately 1.4 meters. The templates are discretized versions of handprinted English capital letters A-Z, with symmetry added during the discretization.

0	0	0	0	0	0	0	0
1	1	1	1	1	1	1	1
2	2	2	2	2	2	2	2
3	3	3	3	3	3	3	3
4	4	4	4	4	4	4	4
5	5	5	5	5	5	5	5
6	6	6	6	6	6	6	6
7	7	7	7	7	7	7	7
8	8	8	8	8	8	8	8

a) Numerical



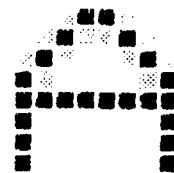
b) Gray Scale
Representation

Figure A-1. Gray Scale Used for Representation of Template Letters.

```

3 8 4 0 0 4 8 8
8 4 0 4 4 0 4 8
4 0 4 8 8 4 0 4
0 4 8 8 8 8 4 0
0 0 0 0 0 0 0 0
0 8 8 8 8 8 8 0
0 8 8 8 8 8 8 0
0 8 8 8 8 8 8 0

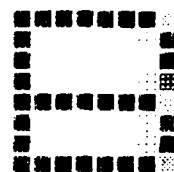
```



```

0 0 0 0 0 0 0 4
0 8 8 8 8 8 7 0
0 8 8 8 8 8 8 0
0 8 8 8 8 8 7 1
0 0 0 0 0 0 0 6
0 8 8 8 8 8 7 0
0 8 8 8 8 8 7 0
0 0 0 0 0 0 0 4

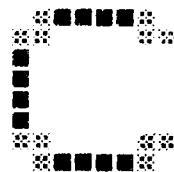
```



```

8 3 0 0 0 0 3 8
3 3 8 8 8 8 3 3
0 8 8 8 8 8 8 8
0 8 8 8 8 8 8 8
0 8 8 8 8 8 8 8
0 8 8 8 8 8 8 8
3 3 8 8 8 8 3 3
8 3 0 0 0 0 3 8

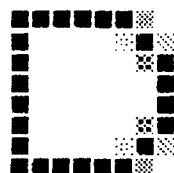
```



```

0 0 0 0 0 0 4 8
0 8 8 8 8 6 0 5
0 8 8 8 8 8 3 0
0 8 8 8 8 8 8 0
0 8 8 8 8 8 8 0
0 8 8 8 8 8 3 0
0 8 8 8 8 6 0 5
0 0 0 0 0 0 4 8

```



```

0 0 0 0 0 0 0 0
0 8 8 8 8 8 8 8
0 8 8 8 8 8 8 8
0 8 8 8 8 8 8 8
0 0 0 0 0 8 8 8
0 8 8 8 8 8 8 8
0 8 8 8 8 8 8 8
0 0 0 0 0 0 0 0

```



a) Numerical

b) Gray Scale
Representation

Figure A-2. Letters Used as Templates.

```

0 0 0 0 0 0 0 0
0 8 8 8 8 8 8 8
0 8 8 8 8 8 8 8
0 8 8 8 8 8 8 8
0 0 0 0 8 8 8 8
0 8 8 8 8 8 8 8
0 8 8 8 8 8 8 8
0 8 8 8 8 8 8 8

```

```

0000000000
0000000000
0000000000
0000000000
0000000000
0000000000
0000000000
0000000000

```

```

8 3 0 0 0 0 3 8
3 3 8 8 8 8 3 3
0 8 8 8 8 8 8 8
0 8 8 8 8 8 8 8
0 8 8 8 8 8 8 8
0 8 8 8 8 8 8 8
0 8 8 8 8 0 0 0
3 3 8 8 8 8 3 3
8 3 0 0 0 0 3 8

```

```

0000000000
0000000000
0000000000
0000000000
0000000000
0000000000
0000000000
0000000000

```

```

0 8 8 8 8 8 8 0
0 8 8 8 8 8 8 0
0 8 8 8 8 8 8 0
0 8 8 8 8 8 8 0
0 0 0 0 0 0 0 0
0 8 8 8 8 8 8 0
0 8 8 8 8 8 8 0
0 8 8 8 8 8 8 0

```

```

0000000000
0000000000
0000000000
0000000000
0000000000
0000000000
0000000000
0000000000

```

```

8 0 0 0 0 0 0 8
8 8 8 1 1 8 8 8
8 8 8 2 2 8 8 8
8 8 8 2 2 8 8 8
8 8 8 2 2 8 8 8
8 8 8 2 2 8 8 8
8 8 8 1 1 8 8 8
8 0 0 0 0 0 0 8

```

```

0000000000
0000000000
0000000000
0000000000
0000000000
0000000000
0000000000
0000000000

```

```

8 8 8 8 8 8 8 0
8 8 8 8 8 8 8 0
8 8 8 8 8 8 8 0
8 8 8 8 8 8 8 0
8 8 8 8 8 8 8 0
1 4 8 8 8 8 4 1
3 0 4 8 8 4 0 3
8 5 0 0 0 0 5 8

```

```

0000000000
0000000000
0000000000
0000000000
0000000000
0000000000
0000000000
0000000000

```

a) Numerical

b) Gray Scale Representation

Figure A-2. Letters Used as Templates.

```

0 8 8 8 8 4 2 0
0 8 8 6 2 0 3 6
0 6 2 0 3 8 8 8
0 0 2 8 8 8 8 8
0 0 2 8 8 8 8 8
0 6 2 0 3 8 8 8
0 8 8 6 2 0 3 6
0 8 8 8 8 4 2 0

```

```

0 8 8 8 8 8 8 8
0 8 8 8 8 8 8 8
0 8 8 8 8 8 8 8
0 8 8 8 8 8 8 8
0 8 8 8 8 8 8 8
0 8 8 8 8 8 8 8
0 8 8 8 8 8 8 8
0 0 0 0 0 0 0 0

```

```

2 0 5 8 8 5 0 2
0 3 0 6 6 0 3 0
0 8 8 0 0 8 8 0
0 8 8 3 3 8 8 0
0 8 8 8 8 8 8 0
0 8 8 8 8 8 8 0
0 8 8 8 8 8 8 0
0 8 8 8 8 8 8 0

```

```

0 4 8 8 8 8 8 0
0 1 8 8 8 8 8 0
0 7 2 4 8 8 8 0
0 8 7 1 4 8 8 0
0 8 8 7 0 7 8 0
0 8 8 8 4 2 8 0
0 8 8 8 8 2 3 0
0 8 8 8 8 7 0 0

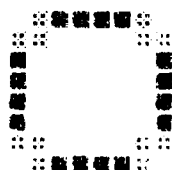
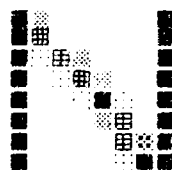
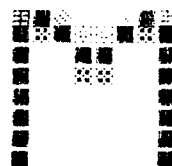
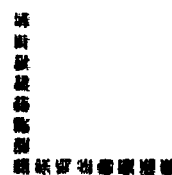
```

```

8 3 0 0 0 0 3 8
3 3 8 8 8 8 3 3
0 8 8 8 8 8 8 0
0 8 8 8 8 8 8 0
0 8 8 8 8 8 8 0
0 8 8 8 8 8 8 0
3 3 8 8 8 8 3 3
8 3 0 0 0 0 3 8

```

a) Numerical



b) Gray Scale Representation

Figure A-2. Letters Used as Templates.

9 0 0 0 0 0 0 3
 0 8 8 8 8 8 7 0
 0 8 8 8 8 8 8 0
 0 8 8 8 8 8 7 0
 0 0 0 0 0 0 0 3
 0 8 8 8 8 8 8 8
 0 8 8 8 8 8 8 8
 0 8 8 8 8 8 8 8

8 3 0 0 0 0 3 8
 3 3 8 8 8 8 3 3
 0 8 8 8 8 8 8 0
 0 8 8 8 8 8 8 0
 0 8 8 8 8 8 8 0
 0 8 8 8 3 0 5 0
 3 3 8 8 8 2 0 3
 8 3 0 0 0 0 1 2

0 0 0 0 0 0 0 3
 0 8 8 8 8 8 7 0
 0 8 8 8 8 8 8 0
 0 8 8 8 8 8 7 0
 0 0 0 0 0 0 0 3
 0 8 8 4 0 4 8 8
 0 8 8 8 4 0 4 8
 0 8 8 8 8 4 0 4

8 3 0 0 0 0 3 8
 3 3 8 8 8 8 3 3
 0 6 8 8 8 8 8 8
 4 0 2 3 5 6 8 8
 8 8 6 5 3 2 0 4
 8 8 8 8 8 8 6 0
 3 3 8 8 8 8 3 3
 8 3 0 0 0 0 3 8

0 0 0 0 0 0 0 0
 8 8 8 1 1 8 8 8
 8 8 8 2 2 8 8 8
 8 8 8 2 2 8 8 8
 8 8 8 2 2 8 8 8
 8 8 8 2 2 8 8 8
 8 8 8 2 2 8 8 8
 8 8 8 2 2 8 8 8

a) Numerical

8 8 8 8 8 8 8 8
 8 8 8 8 8 8 8 8
 8 8 8 8 8 8 8 8
 8 8 8 8 8 8 8 8
 8 8 8 8 8 8 8 8
 8 8 8 8 8 8 8 8
 8 8 8 8 8 8 8 8
 8 8 8 8 8 8 8 8

8 8 8 8 8 8 8 8
 8 8 8 8 8 8 8 8
 8 8 8 8 8 8 8 8
 8 8 8 8 8 8 8 8
 8 8 8 8 8 8 8 8
 8 8 8 8 8 8 8 8
 8 8 8 8 8 8 8 8
 8 8 8 8 8 8 8 8

8 8 8 8 8 8 8 8
 8 8 8 8 8 8 8 8
 8 8 8 8 8 8 8 8
 8 8 8 8 8 8 8 8
 8 8 8 8 8 8 8 8
 8 8 8 8 8 8 8 8
 8 8 8 8 8 8 8 8
 8 8 8 8 8 8 8 8

8 8 8 8 8 8 8 8
 8 8 8 8 8 8 8 8
 8 8 8 8 8 8 8 8
 8 8 8 8 8 8 8 8
 8 8 8 8 8 8 8 8
 8 8 8 8 8 8 8 8
 8 8 8 8 8 8 8 8
 8 8 8 8 8 8 8 8

8 8 8 8 8 8 8 8
 8 8 8 8 8 8 8 8
 8 8 8 8 8 8 8 8
 8 8 8 8 8 8 8 8
 8 8 8 8 8 8 8 8
 8 8 8 8 8 8 8 8
 8 8 8 8 8 8 8 8
 8 8 8 8 8 8 8 8

b) Gray Scale Representation

Figure A-2. Letters Used as Templates.

0	8	8	8	8	8	8	0
0	8	8	8	8	8	8	0
0	8	8	8	8	8	8	0
0	8	8	8	8	8	8	0
0	8	8	8	8	8	8	0
1	4	8	8	8	8	4	1
3	0	4	8	8	4	0	3
8	5	0	0	0	0	5	8

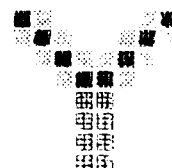
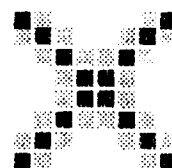
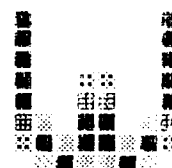
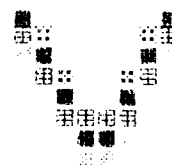
0	6	8	8	8	8	6	0
2	3	8	8	8	8	3	2
4	0	8	8	8	8	0	4
8	2	3	8	8	3	2	8
8	6	0	8	8	0	6	8
6	8	2	2	2	2	8	8
8	8	6	0	0	6	8	8
8	8	8	4	4	8	8	8

0	8	8	8	8	8	8	0
0	8	8	8	8	8	8	0
0	8	8	8	8	8	8	0
0	8	8	3	3	8	8	0
0	8	8	2	2	8	8	0
1	4	8	0	0	8	4	1
3	0	4	0	0	4	0	3
8	5	0	4	4	0	5	8

0	4	8	8	8	8	4	0
4	0	4	8	8	4	0	4
8	4	0	4	4	0	4	8
8	8	4	0	0	4	8	8
8	8	4	0	0	4	8	8
8	4	0	4	4	0	4	8
4	0	4	8	8	4	0	4
0	4	8	8	8	8	4	0

0	4	8	8	8	8	4	0
4	0	4	8	8	4	0	4
8	4	0	4	4	0	4	8
8	8	4	0	0	4	8	8
8	8	8	1	1	8	8	0
8	8	8	2	2	8	8	8
8	8	8	2	2	8	8	8
8	8	8	2	2	8	8	8

a) Numerical



b) Gray Scale Representation

Figure A-2. Letters Used as Templates.

0	0	0	0	0	0	0	0
8	8	8	8	8	7	1	4
8	8	8	8	7	2	3	8
8	8	8	7	1	4	3	3
8	8	4	0	4	8	6	8
7	2	2	7	8	8	3	8
0	3	8	8	8	6	6	6
0	0	0	0	0	0	0	0

a) Numerical

b) Gray Scale
Representation

Figure A-2. Letters Used as Templates.

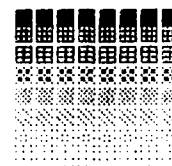
APPENDIX B

The test letters used in this research are shown in numerical and gray scale representation in Figure B-2. The gray scale used for the representations is given in Figure B-1, and ranges from 0 (black) to 8 (white). To observe the representations with the fundamental spatial frequency equal to 1 cycle/degree, the letters should be viewed at a distance of approximately 1.4 meters.

The test letters are variants of the templates given in Appendix A. The test letters consist of an A-to-H transformation (Letter 1 through 5), 10 handprinted letters without symmetry adjustment, and 5 miscellaneous variants.

0	0	0	0	0	0	0	0
1	1	1	1	1	1	1	1
2	2	2	2	2	2	2	2
3	3	3	3	3	3	3	3
4	4	4	4	4	4	4	4
5	5	5	5	5	5	5	5
6	6	6	6	6	6	6	6
7	7	7	7	7	7	7	7
8	8	8	8	8	8	8	8

a) Numerical



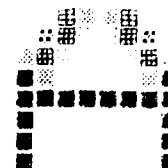
b) Gray Scale
Representation

Figure B-1. Gray Scale Used for Representation of Test Letters.

```

8 8 2 4 4 2 8 8
8 3 1 7 7 1 3 8
4 1 6 8 8 6 1 4
0 4 8 8 8 8 4 0
0 0 0 0 0 0 0 0
0 8 8 8 8 8 8 0
0 8 8 8 8 8 8 0
0 8 8 8 8 8 8 0

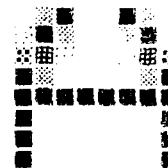
```



```

8 4 0 8 8 0 4 8
6 0 4 8 8 4 0 6
3 1 7 8 8 7 1 3
0 4 8 8 8 8 4 0
0 0 0 0 0 0 0 0
0 8 8 8 8 8 8 0
0 8 8 8 8 8 8 0
0 8 8 8 8 8 8 0

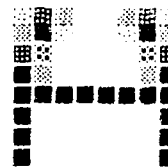
```



```

6 1 4 8 8 4 1 6
4 0 6 8 8 6 0 4
1 3 8 8 8 8 3 1
0 4 8 8 8 8 4 0
0 0 0 0 0 0 0 0
0 8 8 8 8 8 8 0
0 8 8 8 8 8 8 0
0 8 8 8 8 8 8 0

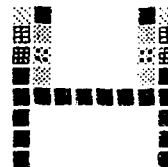
```



```

5 0 8 8 8 8 0 5
2 4 8 8 8 8 4 2
1 3 8 8 8 8 3 1
0 4 8 8 8 8 4 0
0 0 0 0 0 0 0 0
0 8 8 8 8 8 8 0
0 8 8 8 8 8 8 0
0 8 8 8 8 8 8 0

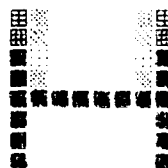
```



```

2 4 8 8 8 8 4 2
1 5 8 8 8 8 5 1
0 7 8 8 8 8 7 0
0 4 8 8 8 8 4 0
0 0 0 0 0 0 0 0
0 8 8 8 8 8 8 0
0 8 8 8 8 8 8 0
0 8 8 8 8 8 8 0

```



a) Numerical

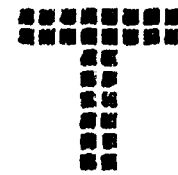
b) Gray Scale
Representation

Figure B-2. Letters Used as Test Inputs.

```

0 0 0 0 0 0 0 0
0 0 0 0 0 0 0 0
8 8 8 0 0 8 8 8
8 8 8 0 0 8 8 8
8 8 8 0 0 8 8 8
8 8 8 0 0 8 8 8
8 8 8 0 0 8 8 8
8 8 8 0 0 8 8 8

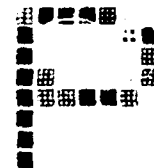
```



```

2 0 0 0 1 4 7 8
0 6 6 6 6 3 0 7
0 7 8 8 8 7 1 5
0 1 8 8 8 5 1 6
0 1 1 0 0 1 5 8
0 7 7 7 8 8 8 8
0 7 8 8 8 8 8 8
0 8 8 8 8 8 8 8

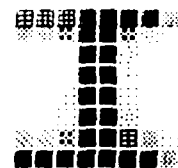
```



```

2 1 1 0 0 0 0 4
4 4 3 0 0 3 6 7
8 8 8 0 0 6 8 8
8 8 8 0 0 7 8 8
8 8 8 0 0 7 8 8
8 8 7 0 0 6 8 8
5 5 3 0 0 2 4 7
0 0 0 0 0 0 0 4

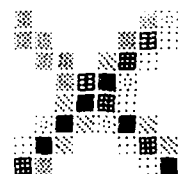
```



```

4 8 8 8 8 8 4 6
4 4 8 8 8 4 2 7
8 4 4 8 5 1 7 8
8 8 4 2 0 6 8 8
8 8 5 0 1 7 8 8
8 6 0 5 6 0 5 8
7 0 5 8 8 7 1 5
1 4 8 8 8 8 7 0

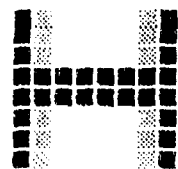
```



```

0 4 8 8 8 8 4 0
0 4 8 8 8 8 4 0
0 4 8 8 8 8 4 0
0 0 0 0 0 0 0 0
0 0 0 0 0 0 0 0
0 4 8 8 8 8 4 0
0 4 8 8 8 8 4 0
0 5 8 8 8 8 4 0

```



a) Numerical

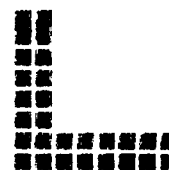
b) Gray Scale Representation

Figure B-2. Letters Used as Test Inputs.

```

0 0 8 8 8 8 8 8
0 0 8 8 8 8 8 8
0 0 8 8 8 8 8 8
0 0 8 8 8 8 8 8
0 0 8 8 8 8 8 8
0 0 8 8 8 8 8 8
0 0 0 0 0 0 0 0
0 0 0 0 0 0 0 0

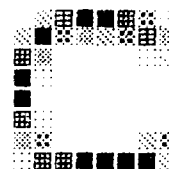
```



```

8 5 2 0 0 1 3 7
5 0 3 4 5 3 2 4
1 4 8 8 8 8 7 6
0 7 8 8 8 8 8 8
0 8 8 8 8 8 8 8
1 7 8 8 8 8 8 8
4 3 8 8 8 8 5 3
7 1 1 0 0 0 0 5

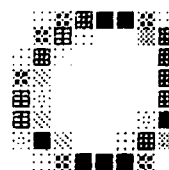
```



```

8 7 3 1 0 0 3 7
8 3 2 7 8 8 4 1
7 1 7 8 8 8 8 1
3 5 8 8 8 8 8 1
2 6 8 8 8 8 8 1
2 5 8 8 8 8 6 0
6 0 5 8 8 7 1 4
8 7 3 0 0 0 3 8

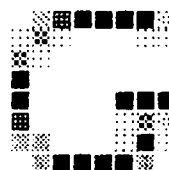
```



```

8 5 1 0 0 0 0 6
7 3 7 8 8 8 7 7
3 7 8 8 8 8 8 8
0 8 8 8 8 8 8 8
0 8 8 8 8 0 0 0
1 8 8 8 8 7 3 6
4 4 8 8 8 7 0 7
8 4 0 0 0 0 4 8

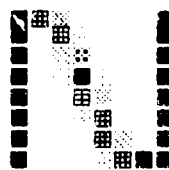
```



```

0 1 4 8 8 8 8 0
0 8 1 6 8 8 8 0
0 8 5 3 8 8 8 0
0 8 7 0 7 8 8 0
0 8 8 2 4 8 8 0
0 8 8 5 1 8 8 0
0 8 8 8 1 5 8 0
0 8 8 8 6 1 0 0

```



a) Numerical

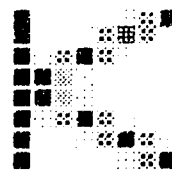
b) Gray Scale
Representation

Figure B-2. Letters Used as Test Inputs.

```

0 8 8 8 8 7 3 0
0 8 8 7 3 1 3 7
0 7 3 0 3 7 8 8
0 0 4 8 8 8 8 8
0 0 4 8 8 8 8 8
0 7 3 0 3 7 8 8
0 8 8 7 3 1 3 7
0 8 8 8 8 7 3 0

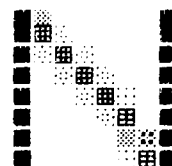
```



```

0 4 8 8 8 8 8 0
0 1 6 8 8 8 8 0
0 6 1 6 8 8 8 0
0 8 6 1 6 8 8 0
0 8 8 6 1 7 8 0
0 8 8 8 6 2 8 0
0 8 8 8 8 4 3 0
0 8 8 8 8 7 2 0

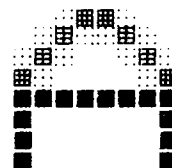
```



```

8 8 7 1 1 7 8 8
8 7 2 7 7 2 7 8
7 2 7 8 8 7 2 7
1 7 8 8 8 8 7 1
0 0 0 0 0 0 0 0
0 8 8 8 8 8 8 0
0 8 8 8 8 8 8 0
0 8 8 8 8 8 8 0

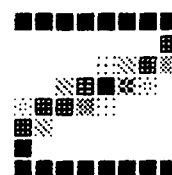
```



```

0 0 0 0 0 0 0 0
8 8 8 8 8 8 8 1
8 8 8 8 7 5 1 4
8 8 5 2 0 3 6 8
6 1 1 4 7 8 8 8
1 5 8 8 8 8 8 8
0 8 8 8 8 8 8 8
0 0 0 0 0 0 0 0

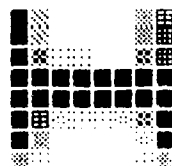
```



```

0 5 8 8 8 8 4 2
0 5 8 8 8 8 4 1
0 3 7 7 8 8 3 1
0 0 0 0 0 0 0 0
0 0 0 0 0 0 0 0
0 2 6 7 7 6 3 0
0 4 8 8 8 8 6 0
4 7 8 8 8 8 7 4

```



a) Numerical

b) Gray Scale Representation

Figure B-2. Letters Used as Test Inputs.

VITA

Daniel Eugene Snyder was born on 7 August 1956 in Springfield, Ohio. He graduated from Springfield Shawnee High School in 1974. He attended Ohio State University from which he received the degree of Bachelor of Science in Electrical Engineering in June, 1979. Upon graduation, he was commissioned in the United States Air Force through the Reserve Officer Training Corps (ROTC) program. He was assigned to the Technical Engineering Branch of the 381st Strategic Missile Wing, McConnell AFB, Kansas. He served as chief of the Technical Engineering Branch from May, 1980 until he entered the School of Engineering, Air Force Institute of Technology, in June, 1982.

Permanent Address: 4333 Willow Run Drive
Beavercreek, Ohio 45430

UNCLASSIFIED

SECURITY CLASSIFICATION OF THIS PAGE

AD-A138039

REPORT DOCUMENTATION PAGE

1a. REPORT SECURITY CLASSIFICATION Unclassified		1b. RESTRICTIVE MARKINGS									
2a. SECURITY CLASSIFICATION AUTHORITY		3. DISTRIBUTION/AVAILABILITY OF REPORT Approved for public release Distribution unlimited									
2b. DECLASSIFICATION/DOWNGRADING SCHEDULE											
4. PERFORMING ORGANIZATION REPORT NUMBER(S) AFIT/GEO/EE/83D-8		5. MONITORING ORGANIZATION REPORT NUMBER(S)									
6a. NAME OF PERFORMING ORGANIZATION AFIT-EN	6b. OFFICE SYMBOL (If applicable)	7a. NAME OF MONITORING ORGANIZATION									
6c. ADDRESS (City, State and ZIP Code) Air Force Institute of Technology Wright-Patterson AFB, Ohio 45433		7b. ADDRESS (City, State and ZIP Code)									
8a. NAME OF FUNDING/SPONSORING ORGANIZATION	8b. OFFICE SYMBOL (If applicable)	9. PROCUREMENT INSTRUMENT IDENTIFICATION NUMBER									
8c. ADDRESS (City, State and ZIP Code)		10. SOURCE OF FUNDING NOS. <table border="1"><tr><td>PROGRAM ELEMENT NO.</td><td>PROJECT NO.</td><td>TASK NO.</td><td>WORK UNIT NO.</td></tr><tr><td></td><td></td><td></td><td></td></tr></table>		PROGRAM ELEMENT NO.	PROJECT NO.	TASK NO.	WORK UNIT NO.				
PROGRAM ELEMENT NO.	PROJECT NO.	TASK NO.	WORK UNIT NO.								
11. TITLE (Include Security Classification) (See Reverse)											
12. PERSONAL AUTHOR(S) Daniel E. Snyder											
13a. TYPE OF REPORT M.S. Thesis	13b. TIME COVERED FROM _____ TO _____	14. DATE OF REPORT (Yr., Mo., Day) December 1983	15. PAGE COUNT 60								
16. SUPPLEMENTARY NOTATION Approved for public release. Distribution unlimited. LYNN E. WOLAYER Dean for Research and Professional Development Air Force Institute of Technology (AFIT) Wright-Patterson AFB, Ohio 45433 76284											
17. COSATI CODES <table border="1"><tr><td>FIELD</td><td>GROUP</td><td>SUB. GR.</td></tr><tr><td>06</td><td>04</td><td></td></tr></table>		FIELD	GROUP	SUB. GR.	06	04		18. SUBJECT TERMS (Continue on reverse if necessary; use block number) Pattern Recognition Character Recognition			
FIELD	GROUP	SUB. GR.									
06	04										
19. ABSTRACT (Continue on reverse if necessary and identify by block number) This research focused on representing the magnitude, phase, and orientation of each two-dimensional spatial frequency component of an input as a three-dimensional vector. An extension of the concept of phasor analysis was developed to facilitate this representation. Using Fourier analysis theory, any input can be considered as the sum of its spatial frequency components. Therefore, the input could be represented by a three-dimensional vector which was the summation of the vector representations of the spatial frequency components. This theory was tested in two phases. First, isolated English capital letters A through Z were discretized using an 8x8 grid intended to simulate an input sensor device. The vectors representing these inputs were examined to insure that the letters were separable											
20. DISTRIBUTION/AVAILABILITY OF ABSTRACT UNCLASSIFIED/UNLIMITED <input checked="" type="checkbox"/> SAME AS RPT. <input type="checkbox"/> DTIC USERS <input type="checkbox"/>		21. ABSTRACT SECURITY CLASSIFICATION Unclassified									
22a. NAME OF RESPONSIBLE INDIVIDUAL Daniel E. Snyder	22b. TELEPHONE NUMBER (Include Area Code) 513-255-5533	22c. OFFICE SYMBOL AFIT/EN									

UNCLASSIFIED

SECURITY CLASSIFICATION OF THIS PAGE

11. Title

ISOLATED CHARACTER RECOGNITION BASED ON THREE-DIMENSIONAL PHASOR
REPRESENTATION OF SPATIAL FREQUENCY COMPONENTS

19. Abstract

and letters which appear as similar to human observers were clustered. Second, twenty test letters were used to test the capability of this scheme in recognizing variants of the templates. Each phase was tested using unfiltered spatial frequency components and components filtered by the modulation transfer function (MTF) of the human visual system, and the vectors were plotted in one of two spaces.

The template letters were separable and similar letters were clustered. The recognition rate ranged from 40% to 60%, depending on the choice of input filter and space used to plot the vectors.

UNCLASSIFIED

SECURITY CLASSIFICATION OF THIS PAGE

FILME
3-84